

Molecular Recognition in Chiral Monolayers of Stearoylserine Methyl Ester

Noel G. Harvey, Dorla Mirajovsky, Philip L. Rose, Robert Verbiar, and Edward M. Arnett*

Contribution from the Department of Chemistry, Duke University, Durham, North Carolina 27706. Received July 11, 1988

Abstract: An in-depth study of the surface properties of the enantiomers of stearylserine methyl ester and their mixtures is presented. Force/area isotherms and equilibrium spreading pressures at several temperatures yield thermodynamic properties for spreading from the crystalline enantiomers or racemate. Hysteresis in compression/expansion cycles and surface viscosities demonstrate that relaxation between metastable surface states is relatively slow. All of the above properties show strongly temperature-dependent chiral recognition, which is attributed primarily to long-range order in the quasicrystalline enantiomeric films relative to the highly fluid, well-mixed racemic ones. Visualization of the films by epifluorescent microscopy (in situ on the surface), transmission electron microscopy, and scanning tunneling microscopy support, but do not prove, this interpretation.

The selective interaction of molecules through properly oriented functionalities has been a matter of long-standing interest to organic chemists and is presently enjoying increased attention and refinement under the rubric "molecular recognition". A wide variety of host molecules have been designed¹⁻³ to selectively entrap ions of different sizes or to provide carefully engineered clefts or pockets which may capture neutral species by such intermolecular forces as hydrogen bonding, aromatic stacking interactions, or dipole-dipole forces. The model of perfection for molecular recognition is the extreme specificity of enzyme-substrate interactions, which takes added advantage of chiral recognition to enhance host-guest recognition.

Chiral discrimination at surfaces has been developed especially through the leadership of Pirkle,⁴ and a wide variety of chiral stationary phases (CSPs) have been invented for the resolution of racemic mixtures through diastereomeric interactions between the CSP and enantiomers dissolved in the mobile phase. The rational approach for the design of CSPs has considered that molecular recognition to form diastereomeric complexes between the chiral elements of the functionalized surface and those in the mobile phase takes place through a three-point interaction between appropriate polar, aromatic, or hydrogen-bonding functions similar to opposed tripods touching in a plane. In the case of CSPs the chiral host's functionalities are preoriented by virtue of its attachment to a surface. Host molecules in homogeneous media depend on carefully constructed preorganized rings, cavities, or clefts for the capture of the guest molecule. Both of these arrangements suffer from a common deficiency—there is no way other than variation of concentration or solvent of manipulating the molecular recognition process once the CSP or host molecule has been prepared. There is, however, a unique area of surface chemistry in which the packing forces and geometric orientation of molecules at an interface can be varied at will. The techniques of monolayer study developed primarily by Langmuir,⁵ Harkins,⁶ Adam,⁷ and their colleagues provide an unparalleled opportunity to manipulate the orientation (and even conformation) of molecules under conditions of sharply defined geometric arrangement. When amphiphathic molecules are spread as a monolayer on the surface of water in a Langmuir film balance, the intermolecular packing forces and the orientation of hydrocarbon chains can be controlled

by variation of the area containing the monolayer.

If the surface-active molecules which form the monolayer on the water surface are also chiral, there is an opportunity to study stereospecific molecular recognition by taking advantage of the preorganization of the chiral elements in the surfactant by the surface. One may imagine a surfactant molecule with a chiral headgroup as having three different functionalities of varying polarity associated with the water surface, with the hydrocarbon chain excluded from the water surface by the hydrophobic effect.⁸ The three groups in the surface represent a tripod at the points of the triangular base of the tetrahedron generated around the asymmetric carbon at the center of chirality (Figure 1).

Strong, shape-dependent short-range forces in the crystals of chiral substances result in the familiar stereodifferentiation of unit-cell structures and lattice energies between enantiomers and their racemic mixtures or between diastereomeric mixtures. In contrast, stereoselectivity in the properties of mixed chiral liquids is barely measurable.^{9,10} It is reasonable to suppose that chiral recognition might be strongly expressed in mixtures of chiral surfactants which are preorganized in monolayers on a water surface and then subjected to lateral compression with a Langmuir film balance. Although "gaseous" or "liquid" monolayer states have relatively weak interactions between surfactant molecules, highly compressed states with small areas/molecule may approach the packing requirements of crystals and therefore exhibit chiral molecular recognition, although there is no guarantee that the associations within a closely packed film are the same or even similar to those in the bulk crystalline phase. We have demonstrated previously that such "molecular recognition" may occur in films cast from enantiomers and their racemic mixture.¹¹⁻¹³ More recently, we have shown that such recognition is reflected directly in the thermodynamics of mixing for a series of diastereomeric surfactants confined to the air/water interface.^{14,15}

The present article relates an in-depth study of stearylserine methyl ester, the amino acid derivative which in our hands has exhibited the most pronounced chiral recognition phenomena through a variety of surface properties.¹⁶ In addition to the

- (1) Rebek, J. *Science* **1987**, *235*, 1478.
- (2) Rebek, J.; Askew, B.; Killoran, M.; Nemeth, D.; Lin, F. T. *J. Am. Chem. Soc.* **1987**, *109*, 2426.
- (3) Rebek, J.; Marshall, L.; Wolak, R.; Parriss, K.; Killoran, M.; Askew, B.; Nemeth, D.; Islam, N. *J. Am. Chem. Soc.* **1985**, *107*, 7476.
- (4) (a) Pirkle, W. H.; Hyun, M. H.; Bank, B. *J. Chromatog.* **1984**, *316*, 585. (b) Wainer, I. W. *TrAC, Trends Anal. Chem. (Pers. Ed.)* **1987**, *6*, 125.
- (5) Langmuir, I. *J. Am. Chem. Soc.* **1917**, *39*, 1869.
- (6) Harkins, W. D. *J. Am. Chem. Soc.* **1917**, *39*, 541.
- (7) Adam, N. K.; Jessop, G. *Proc. R. Soc. London A* **1926**, *A110*, 423.

(8) Tanford, C. *The Hydrophobic Effect: Formation of Micelles and Biological Membranes*; Wiley: New York, 1973.

(9) Atik, Z.; Ewing, M. B.; McGlashan, M. L. *J. Phys. Chem.* **1981**, *85*, 3300.

(10) Atik, Z.; Ewing, M. B.; McGlashan, M. L. *J. Chem. Thermodyn.* **1983**, *15*, 159.

(11) Arnett, E. M.; Chao, J.; Kinzig, B.; Stewart, M.; Thompson, O. *J. Am. Chem. Soc.* **1978**, *100*, 5575.

(12) Arnett, E. M.; Thompson, O. *J. Am. Chem. Soc.* **1981**, *103*, 968.

(13) Arnett, E. M.; Chao, J.; Kinzig, B.; Stewart, M.; Thompson, O.; Verbiar, R. *J. Am. Chem. Soc.* **1982**, *104*, 389.

(14) Harvey, N.; Rose, P. L.; Porter, N. A.; Huff, J. B.; Arnett, E. M. *J. Am. Chem. Soc.* **1988**, *110*, 4395.

(15) Arnett, E. M.; Harvey, N.; Rose, P. L. *Langmuir* **1988**, *4*, 1049.

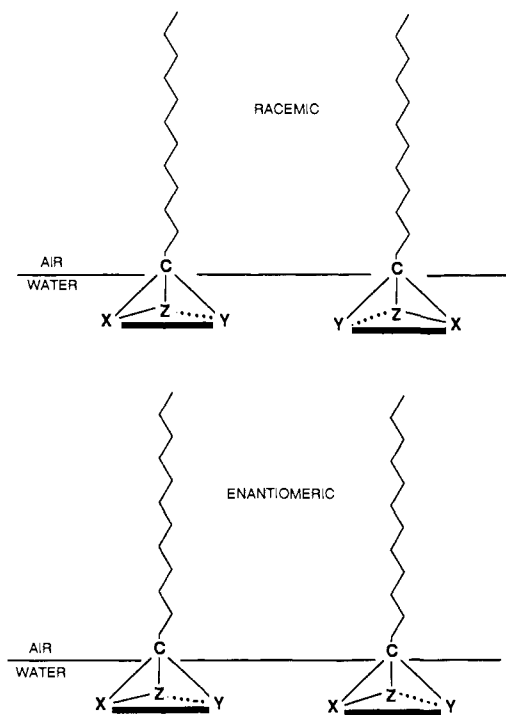


Figure 1. Idealized chiral surfactants with headgroups oriented in the air/water interface to produce enantiomeric triangles on the surface. The three substituents, X, Y, and Z, about the chiral center form a triangular base; interactions between sides of the triangles are different for a pair of homochiral enantiomers than for the heterochiral racemic pair.

familiar force/area isotherms at several temperatures, we will present here an extensive study of surface spreading, mixing properties, surface viscosity, and hysteresis of the monolayer films and compare these properties to those of the bulk crystals. Finally, these will be related to microscopic observations of the films both in situ at the air/water interface by means of epifluorescent microscopy and by scanning tunneling microscopy of Langmuir-Blodgett transferred films.

Experimental Section

Materials Preparation and Purification. Stearoylserine methyl esters were prepared by coupling the serine methyl esters with stearoyl chloride by using the method of Zeelen and Havinga.¹⁶ (*S*)-(+)-, (*R*)-(-)-, and (*R,S*)-(\pm)-serine methyl ester hydrochlorides (Sigma) were recrystallized twice from distilled methanol/ether before use. Stearic acid (United States Biochemical Corp.) used to prepare stearoyl chloride was recrystallized 6–10 times from distilled ethanol. Its purity (>99.9%) was determined by GLPC analysis of the corresponding methyl ester as described previously.¹³ Conversion into stearoyl chloride was accomplished with PCl_5 in CCl_4 .¹⁷ The stearoylserine methyl esters were then obtained by condensing the stearoyl chloride with the serine methyl ester hydrochloride in a chloroform/aqueous KHCO_3 system. They were recrystallized 10–12 times from ethyl acetate/methanol solvent mixtures and showed only one spot by TLC analysis in a 115:45:4:4 $\text{CHCl}_3/\text{MeOH}/\text{H}_2\text{O}/\text{NH}_4\text{OH}$ eluting solvent mixture. The melting point of the *S*-(+) and *R*-(-) isomers was 89.8–90.5 °C, while that of the racemic mixture was 93.5–94.0 °C. As a general precaution for the conservation of optical and chemical purity, all glassware used in these syntheses was cleaned as described previously.^{11–13}

Structures of the stearoylserine methyl esters were confirmed by ¹³C and ¹H NMR and IR spectroscopy. Numerous attempts to prepare crystals suitable for X-ray crystallography failed. The IR spectra of the enantiomers were identical, while that of the racemate was noticeably different. The characteristic IR absorption bands are as follows: *R*-(-) or *S*-(+) (cm^{-1}), 3520 (OH), 3000 (NH), 1725 (ester CO), 1625 (amide I), 1545 (amide II), 1468, 1458 (amide CH, CH_2), 1435 (ester OCH_3);

R,S-(\pm) (cm^{-1}), 3490 (OH), 3000 (NH), 1725 (ester CO), 1645 (amide I), 1545 (amide II), 1463, 1415 (amide CH, CH_2), 1435 (ester OCH_3).

Melting Point Diagram. The melting point/composition diagram for mixtures of (*S*)-(+)- and (*R*)-(-)-stearoylserine methyl ester was determined with a Thomas-Hoover capillary melting point apparatus. Crystals of a fixed *S*-(+) to *R*-(-) ratio were prepared by weighing 4–5 mg of each enantiomer to the nearest μg on a Cahn RG electrobalance, dissolving each isomer in distilled 9:1 hexanes/ethanol, and diluting to 25 mL in hand-calibrated volumetric flasks. Crystals of the desired enantiomeric composition were then formed by aliquoting the calculated amount of *S*-(+) or *R*-(-) solution into a small (10 mL) round-bottom flask via an Agla microliter syringe and heating the mixture to about 45 °C. Subsequent cooling resulted in the slow crystallization of the mixed solid. After evaporation of the supernatant solvent, the crystals were dried in vacuo at 50 °C for 8 h before melting points were determined.

Differential Scanning Calorimetry. The thermal phase transition temperatures and enthalpies were determined with a DuPont Instruments 1090 Thermal Analyzer. Samples of 5–7 mg were sealed in copper-coated aluminum DSC pans and were equilibrated thermally against an air blank at the starting temperature of 20 °C. The heating thermograms were obtained in the 20–150 °C range at scan rates of 10 and 20 °C/min. The heating-curve areas were measured directly by a DuPont 1090 analysis program.

Langmuir Film Balance Techniques. In view of the constant threat of contamination of both the chiral surfactant and the instruments used to gather these data, every precaution was taken to ensure the cleanliness of each experimental component. These preventive routines have been described in detail.¹³

The automated Langmuir film balance employed here is of the torsion head/floating barrier type, and is sensitive to ± 0.005 dyn/cm. The construction and specifications of the balance have been described in detail.¹³

For all experiments, the subphase water was purified by reverse osmosis and ion exchange and was then twice distilled at pH = 5.5 as described previously.¹³

Crystals of the highly purified enantiomers and racemate of the stearoylserine methyl ester were weighed out to 2–3 mg on a Cahn RG electrobalance and then dissolved in carefully distilled 9:1 hexanes/ethanol spreading solvent. In general, the racemic form took longer (~10 h) to dissolve than either of the enantiomeric forms (~3 h) at room temperature. These solutions were diluted to 25.00 ± 0.001 mL in hand-calibrated volumetric flasks, and aliquots were delivered to the clean air/water interface via an Agla microliter syringe. A regular run consisted of delivering 4.403×10^{16} molecules to an overall area of 6.84×10^{18} Å², or 120 Å²/molecule. In addition, runs were performed in which the films were spread to greater than 1000 Å²/molecule. No difference was observed between those spread to different surface densities. The spreading solvent was allowed to dissipate for 5–20 min before film compression; no difference was noted between pressure–area isotherms that were taken after 5 min and those that were taken after 35 min. Each experiment was repeated 5–12 times from several different sets of solutions.

Spreading solutions of various enantiomeric compositions were prepared as described previously.¹⁵

The stabilities of the films were checked by compressing to a given surface pressure and halting compression; the film was judged “stable” if the surface pressure fell no more than 0.1 dyn $\text{cm}^{-1} \text{min}^{-1}$.^{14,15}

The compression rate was varied from 7.7 to 29.8 Å² molecule⁻¹ min⁻¹; neither the stable portion of the Π/A curve nor the monolayer stability limit was changed by this variation. All isotherms reported here are for a compression rate of 29.8 Å² molecule⁻¹ min⁻¹.

Surface Shear Viscosity. A detailed description of the surface shear canal viscometer and the methods for its use have been given recently.¹⁴ Subphase water was kept at a constant surface temperature to within ± 0.5 °C by means of a serpentine glass circulating coil placed on the trough floor. The entire viscometer assembly is enclosed within a heated temperature control box capable of maintaining the air temperature to within ± 1.0 °C in the 25–40 °C range.

The surface shear viscosities of the enantiomeric and racemic stearoylserine methyl ester films were determined at $\Pi = 2.5$ and 5.0 dyn/cm in the above temperature range. The films were spread by delivering several drops of spreading solution to a large enough surface area to give a very low (0.1 dyn/cm) surface pressure. After allowing 5–10 min for solvent dissipation, the films were compressed to the desired surface pressure. They were allowed to equilibrate for another 5 min before isobaric flow through the surface canal was begun. Each experiment was reproduced 5–12 times, with 5–6 min allowed for film flow.

Newtonian flow of the films was checked by comparing the viscosities of each film with variations in the canal width in the 0.10–0.25-cm range. When the flow was uniform throughout the duration of the measurement

(16) (a) Zeelen, F. J. Ph.D. Dissertation, The State University of Leiden, Leiden, The Netherlands, 1956. (b) Zeelen, F. J.; Havinga, E. *Recl. Trav. Chim. Pays-Bas* **1958**, *77*, 267.

(17) Youngs, C. C.; Epp, A.; Craig, B. M.; Sallans, H. R. *J. Am. Oil Chem. Soc.* **1957**, *34*, 107.

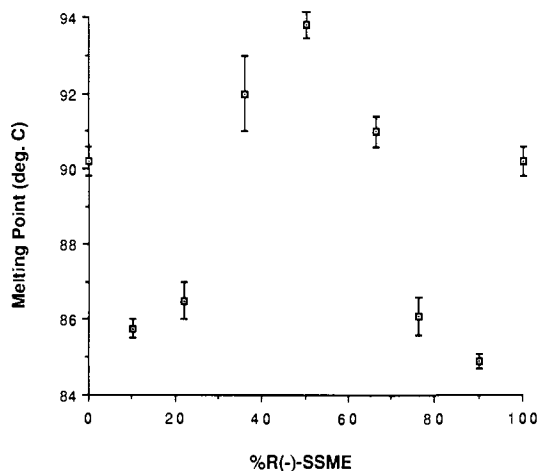


Figure 2. Melting point vs composition diagram for stearylserine methyl ester crystals.

and independent of the shear rate (canal width), the flow was judged to be Newtonian.

Equilibrium Spreading Pressures. ESPs of the surfactants were determined on pure water at 25–40 °C with the Langmuir film balance as described previously.¹²

Langmuir–Blodgett Transferred Films. Langmuir–Blodgett (L–B) films of enantiomeric and racemic stearylserine methyl ester were built up on hydrophobic graphite surfaces by using a homemade L–B apparatus of familiar design.¹⁸

Films were deposited on carbon-film coated EM grids (EM Sciences, CF 100-Cu) and pyrolytic graphite monochromator surfaces (Union Carbide, ZYB grade, 1 cm²). The films were first spread on the water surface, equilibrated for 15 min, and then slowly compressed to the desired surface pressure of 5.0 dyn/cm. The hydrophobic grids were then dipped slowly (5 mm/min) through the film-covered interface and immediately pulled back up through the surface layer. This process occurred with a transfer ratio of about 0.95 and presumably left behind a dry bilayer having a headgroup/headgroup orientation and a hydrophobic surface.

Microscopy. The original in situ epifluorescence micrographs were obtained for us by Professor Harden McConnell's group at Stanford University using a Zeiss epifluorescence microscope and SIT TV-camera system as described previously.¹⁹ Spreading solutions for direct film observations were prepared by inclusion of 2 mol % of the fluorescent probe molecule L-NBD PC (3-acyl-2(R)-[[N-(7-nitro-2,1,3-benzoxadiazol-4-yl)amino]caproyl]glycero-1-phosphocholine, Avanti Polar Lipids). The probe surfactant was recrystallized from chloroform and lyophilized, and solutions of probe were formed in triply distilled chloroform. Mixtures of probe and stearylserine methyl ester (SSME) were formed by introducing aliquots of L-NBD PC into SSME solutions in the same manner as described above. The effect of the probe on the monolayer Π/A properties was gauged by incorporating successive amounts of L-NBD PC into the film. No discernible difference due to probe incorporation as reflected by the Π/A isotherm in either the enantiomeric or racemic films was found up to concentrations of 5 mol % L-NBD PC.

Transmission electron micrographs of L–B films pulled onto EM grids were obtained on a Philips E.M. 300. No stains or fixatives were used on the samples. Scanning tunneling electron micrographs of L–B films pulled onto pyrolytic graphite monochromators were obtained on a Digital Instruments NanoScope II outfitted with a type "B" head. The samples were scanned at a rate of 26 Hz with a bias voltage of 75.1 mV and a tunneling current of 756.8 pA.

Results

Crystalline Solids. It is apparent from the IR spectra and melting points of the racemic and enantiomeric crystals of SSME that solid-phase molecular interactions are differentiated stereochemically. This is highlighted by the melting point vs composition phase diagram (Figure 2) obtained for the mixed crystals. The solid/liquid phase coexistence line for these mixtures is indicative of a racemic compound or racemate in which the smallest unit consists of a heterochiral pair of molecules.²⁰

Table I. Heats and Entropies of Fusion for Crystalline Stearylserine Methyl Ester^a

sample	transition temp, K	ΔH°_f , kcal/mol	ΔS°_f , cal/K mol
(S)-(+)- or (R)-(-)-stearylserine methyl ester	362.1	23.0 ± 1.3	-63.5 ± 4.0
(R,S)-(\pm)-stearylserine methyl ester	367.2	16.4 ± 1.5	-45.0 ± 4.1

$$^a \Delta S_f = \Delta H_f / T_f.$$

Table II. Monolayer Stability Limits, Π_L

T, °K	Π_L , dyn/cm	
	racemic	enantiomeric
293	unstable at all Π	unstable at all Π
298	2.5	unstable at all Π
303	1.5	0.5
313	~21	~19

The thermal phase transition enthalpies and temperatures were studied by differential scanning calorimetry, and the results are tabulated in Table I. Large differences in the melting behavior were observed between the racemic and enantiomeric crystals, with the racemic crystals having a lower enthalpy of fusion despite a higher melting point. In addition, the main transition in the racemate was broad in comparison to the sharp peak of the enantiomer. No other phase transitions were noted.

Π/A Isotherms of Spread Monolayers. The compression/expansion Π/A isotherms of racemic and enantiomeric SSME are shown in Figure 3a–d. It is immediately apparent that chiral discrimination is expressed and is temperature dependent. For example, at 25 °C, the racemic film is more highly expanded at every surface pressure than the enantiomeric film, indicating a more efficient packing in the latter. At lower surface pressures, the difference between racemic and enantiomeric compression/expansion cycles decreases with increasing temperature. At 40 °C, the Π/A isotherms of racemic and enantiomeric SSME are identical up to ~22 dyn/cm. At 20 °C, the chiral discrimination is decreased to the point where the differences in the isotherms are within experimental error.

In nearly every case, the compression/expansion cycles are not coincident, indicating that film-relaxation processes are not on the same time scale as the compression/expansion cycle. Indeed, at every compression/expansion rate studied in the 7.7–29.8 Å² molecule⁻¹ min⁻¹ range, substantial hysteresis was observed. The only exception to this is the racemic film at 40 °C.

The monolayer stability limits as determined by stepwise compression of the film are given in Table II. In every case above 20 °C, the racemic films are stable to higher surface pressures than the films of the individual enantiomers. When compressed to surface pressures less than this limit, the compression/expansion curves are coincident and independent of stereochemistry. Comparison of these data with the ESPs in Table III show that these stability limits correlate closely with crystal = film equilibrium spreading pressures at 25 and 30 °C for the enantiomeric film and at 25 °C for the racemic film. At 30 °C and above, the racemic monolayer appears to be metastable with respect to the bulk phase. At 40 °C, both the racemic and enantiomeric films are stable at surface pressures greater than their equilibrium spreading pressures. In general, compression to Π greater than the stability limit resulted in a rapid loss of surface pressure (> 1.0 dyn cm⁻¹ min⁻¹), presumably to form surface microcrystals. In every case, the surface pressure relaxed back to the ESP or to some surface pressure above the ESP if the film was compressed significantly past equilibrium.

Surface Shear Viscosity. Surface shear viscosities of racemic and enantiomeric SSME monolayers are given in Table IV. At 40 °C, the Newtonian viscosity is independent of stereochemistry at both 2.5 and 5.0 dyn/cm surface pressure. At 35 °C, this is

(18) Blodgett, K. B.; Langmuir, I. *Phys. Rev.* **1937**, *51*, 964.

(19) McConnell, H. M.; Tamm, L. K.; Weis, R. M. *Proc. Natl. Acad. Sci. U.S.A.* **1984**, *81*, 3249.

(20) Eliel, E. L. *Stereochemistry of Carbon Compounds*; McGraw-Hill: New York, 1962; pp 43–47.

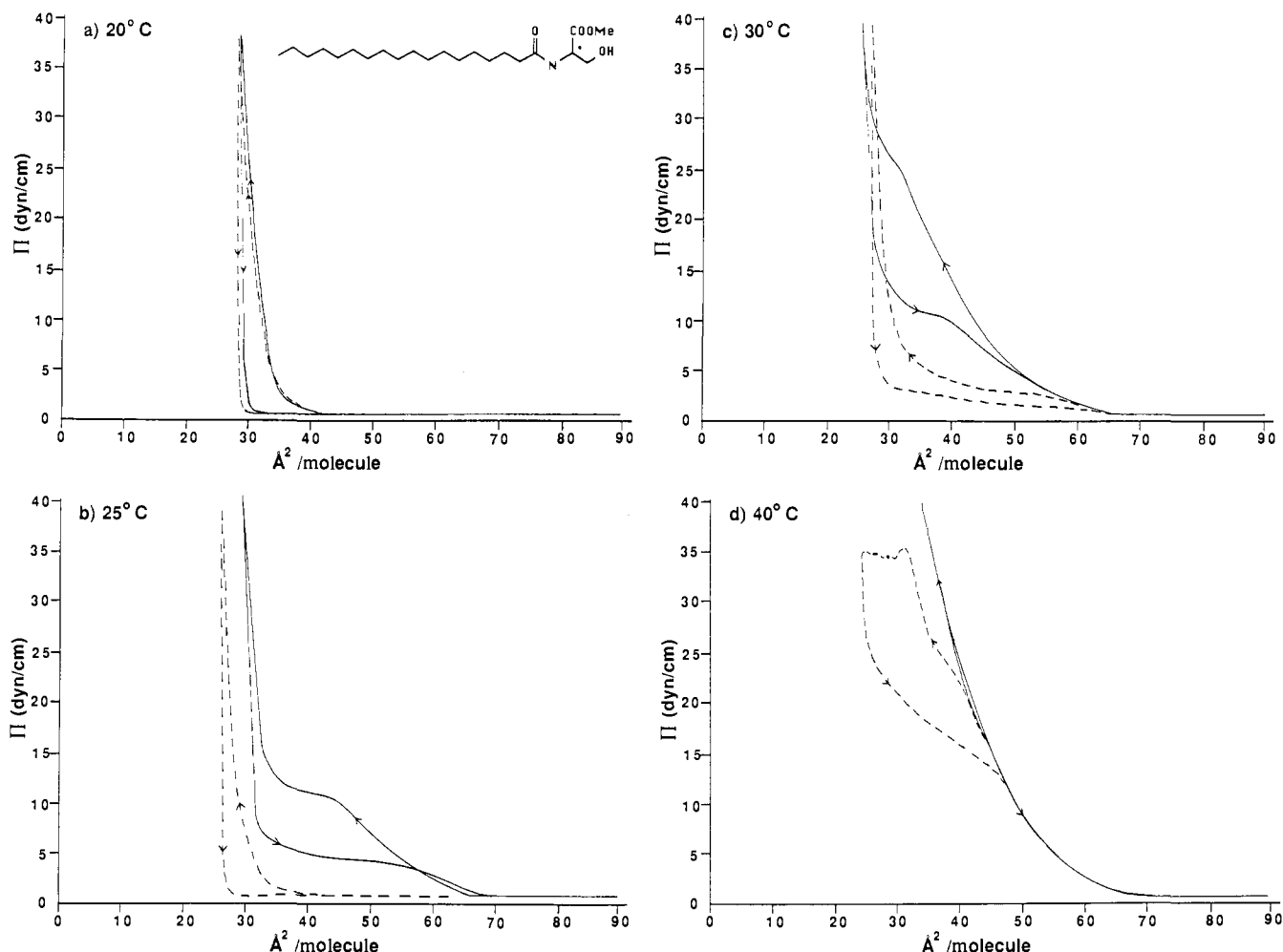


Figure 3. Surface pressure/area isotherms for the compression/expansion cycle of (---) enantiomeric and (—) racemic SSME monolayers on pure water at 20, 25, 30, and 40 °C. The compression rate is $29.8 \text{ \AA}^2 \text{ molecule}^{-1} \text{ min}^{-1}$.

Table III. Equilibrium Spreading Pressures and Surface Free Energies, Enthalpies, and Entropies of Spreading for the Resulting Film

temp, K	Π^e , dyn/cm		A^e , $\text{\AA}^2/\text{molec}$		ΔG^e , kcal/mol		ΔS^e , cal/K mol		ΔH^e , kcal/mol	
	<i>R,S</i> -(±)	<i>R</i> -(-) or <i>S</i> -(+)	<i>R,S</i> -(±)	<i>R</i> -(-) or <i>S</i> -(+)	<i>R,S</i> -(±)	<i>R</i> -(-) or <i>S</i> -(+)	<i>R,S</i> -(±)	<i>R</i> -(-) or <i>S</i> -(+)	<i>R,S</i> -(±)	<i>R</i> -(-) or <i>S</i> -(+)
293										
298	2.5 ± 0.3		58 ± 3		-0.21 ± 0.03		47 ± 4	44 ± 4	14.3 ± 1.2	13.3 ± 1.2
303	4.2 ± 0.3	0.5 ± 0.2	54 ± 2	64 ± 3	-0.33 ± 0.03	-0.05 ± 0.02				
313	11.3 ± 1.5	5.7 ± 0.7	49 ± 2	54 ± 4	-0.77 ± 0.11	-0.44 ± 0.06				

Table IV. Surface Shear Viscosity^a

<i>T</i> , K	$\Pi = 2.5 \text{ dyn/cm}$		$\Pi = 5.0 \text{ dyn/cm}$	
	racemic	enantiomeric	racemic	enantiomeric
293, 298	<i>b</i>	<i>b</i>	<i>b</i>	<i>b</i>
303	0.553 ± 0.026	2.00 ± 1.11^c	0.573 ± 0.42	No flow
308	0.472 ± 0.026	0.504 ± 0.038	0.535 ± 0.040	0.666 ± 0.109^c
313	0.419 ± 0.047	0.393 ± 0.036	0.507 ± 0.039	0.493 ± 0.020

^aSurface viscosity in millisurface poise. ^bCondensed films, no surface flow. ^cMeasurable non-Newtonian flow.

true only at $\Pi = 2.5 \text{ dyn/cm}$; the enantiomeric film viscosity is non-Newtonian at $\Pi = 5.0 \text{ dyn/cm}$. Only the racemic film has a Newtonian viscosity at both surface pressures at 30 °C. Both films are too condensed to flow at 20 and 25 °C.

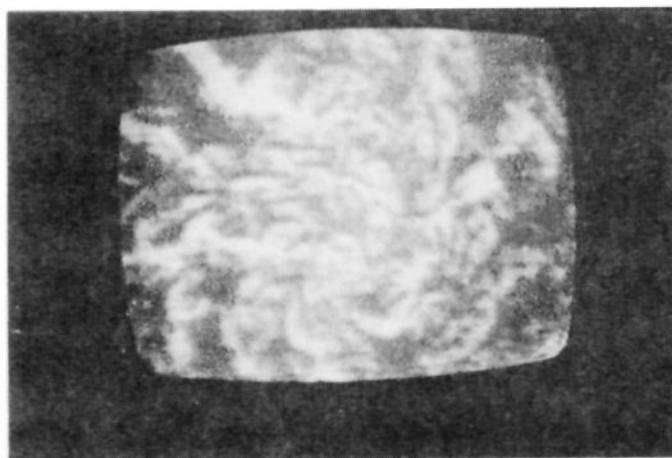
Microscopy and Visualization of Surface Domains. Figure 4 shows the epifluorescence micrographs of enantiomeric and racemic monolayers of SSME (containing 2% fluorescent probe) on the air/water interface at surface pressures of about 0–4 dyn/cm at room temperature. It is clear that the racemic film consists of an array of SSME domains (dark patches) which display no long-range order. In general, these patches begin to

form at around 1 dyn/cm and begin to coalesce upon compression to more than 5–6 dyn/cm. Although an ordering is represented by the rotational character of collections of these domains, inspection of several regions within the film indicates no real preference for clockwise or counter-clockwise rotation such as might be expected if spontaneous resolution were occurring at the interface.¹⁹

In sharp contrast, films cast from enantiomeric material show no such domain formation; at every surface pressure the image consists of a single, highly condensed surface phase. It is difficult to tell exactly when the solid domain forms, since the fluorescent image shows no domain formation until average molecular areas close to the "liftoff" point of the Π/A isotherm are reached. These results contrast with those obtained in the liquid-expanded/liquid-condensed phase transition region of DPPC films, where *R* and *S* films showed a definite chiral ordering in condensed domains.²¹

As the films are compressed past their individual stability limits, collapse to the bulk phase occurs and little information can be

a) RACEMIC



b) ENANTIOMERIC

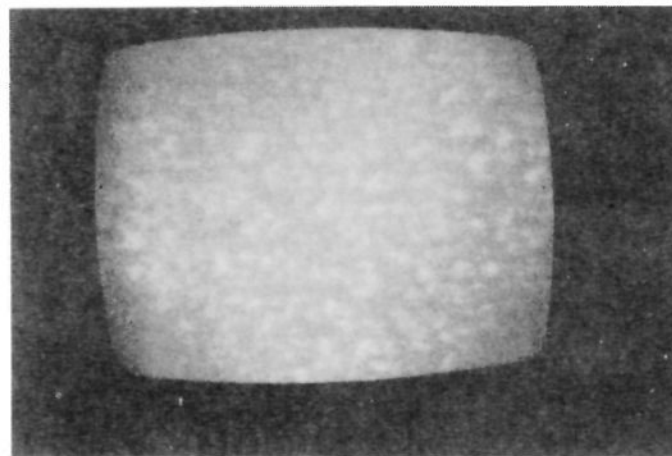


Figure 4. In situ epifluorescence micrographs of (a) "fluid" racemic and (b) "crystalline" enantiomeric SSME monolayers at the air/water interface at 25 °C. Lighter domains are fluorescing probe L-NBD PC; darker domains are SSME. Total magnification is $\sim 5000\times$.

gleaned about three-dimensional collapsed structures with this contrast technique. With this in mind, Langmuir-Blodgett films of both racemic and enantiomeric SSME were pulled at surface pressures above their monolayer stability limits at 25 °C for microscopic observation. Figure 5 shows collapsed domains within the monolayer matrix transferred onto a carbon-film coated EM grid. These domains are apparently composed of "sheets" which have collapsed on top of each other when the film at the air/water interface was compressed to an *apparent* surface pressure of 5 dyn/cm. There appears to be no dependence of microcrystalline domain shapes on stereochemical packing, as has been observed for collapsed structures in condensed phases of 12-hydroxystearic acid.²² Closer inspection of the enantiomeric crystal shows an ordered pattern of striation (or "corrugation") in individual sheets. These are noticeably absent in the collapsed racemic films, which instead contain small darker patches regularly spaced throughout each sheet. Electron diffraction patterns of both reveal a common hexagonal closest-packed pattern (not shown).

Observation via scanning tunneling microscopy of L-B films pulled onto graphite-monochromator surfaces gives an even better idea of the packing differences between racemic and enantiomeric collapsed structures (Figure 6). The ordered domains in the enantiomeric system consist of "rows" of molecules approximately 100 Å across and 35 Å deep, indicating domains that are perhaps 2–3 molecules thick and one molecule deep *at the surface*. The racemic domains show no such ordering; indeed, we have failed to determine any definite pattern in these domains.

Thermodynamics of Spreading from Crystals. Table III gives the thermodynamic properties of spreading from both racemic and enantiomeric crystals. These quantities were derived from the relationships²³

$$\Delta G_s^\circ = -\Pi^c A^c$$

$$\Delta S_s^\circ = A^c d\Pi^c/dT$$

$$\Delta H_s^\circ = \Delta G_s^\circ + T\Delta S_s^\circ = T A^c d\Pi^c/dT - \Pi^c A^c$$

where A^c is the area/molecule at the ESP (Π^c) as obtained from the Π/A isotherm. These properties are calculated from the ESP dependence on temperature. In all cases, ΔG_s° is small and negative, being 0.28 ± 0.04 and 0.33 ± 0.12 kcal/mol (at 30 and 40 °C, respectively) more spontaneous for the racemate.

Within experimental error (which is high due to propagation of error in the term $\Delta G_s^\circ = \Delta H_s^\circ - T\Delta S_s^\circ$), spreading of the racemic and enantiomeric systems requires the same amount of heat, and spreading of the film from the crystal resulted in the same increase in surface entropy. It is impossible to determine from these data whether the differences in ΔG_s° are due to enthalpic or entropic contributions. These results for ΔH_s° and ΔS_s° are different than those which we reported for *N*-(α -methylbenzyl)stearamide, where the enantiomeric spreading resulted in higher values.¹³

Area vs Composition Diagrams. When the molar composition of a binary monolayer is varied, the expression for ideal mixing and, unfortunately, also for complete segregation of the components is given by²⁴

$$A_{12} = n_1 A_1 + n_2 A_2$$

where n_1 and n_2 are the mole percent of components 1 and 2 (the sum of which equals unity) and A_1 and A_2 are the average areas/molecule in the stable, individual films of components 1 and 2 at a fixed surface pressure. Any deviation from this line indicates nonideal interaction, and A_1 may or may not equal A_2 . Similar additive relationships are observed for other monolayer properties, such as first-order phase transition, shear viscosity, and surface potential.²⁴

A unique situation arises when the film components are enantiomers. In this case, A_1 always equals A_2 if the enantiomers 1 and 2 are chemically and optically pure, and a horizontal line will always result if the enantiomers are either ideally mixed or segregated (i.e. spontaneous resolution) into homochiral domains at *any* enantiomeric composition so long as both homochiral and heterochiral domains are of the same phase (i.e., "solid" or "liquid"). Any deviation from this linear relationship indicates, at fixed surface pressure, either nonideal interaction between enantiomers or enantiomorphous phase separation into condensed, solid domains as opposed to fluid monolayer domains. The latter phase separation must be ultimately temperature dependent or kinetic in origin according to the theoretical treatment of enantiomorphous crystallization given by Schipper and Harrowell.²⁵

Figure 7 shows the average area/molecule at "liftoff" vs composition diagram for mixtures of SSME enantiomers in monolayers. The "liftoff" area was chosen for study since it is the first point at which the film components clearly begin to exhibit stereoselective packing in a *condensed* (liquid or solid) monolayer phase. At larger areas/molecule (liftoff to 220 Å²/molecule), the surface pressure remained in the 0.10–0.08 dyn/cm range for all compositions and appeared to follow no discernible trend.²⁶ At surface pressures greater than that at liftoff, the films having an enantiomeric excess of greater than 50% were unstable at $\Pi \gtrsim 0.90$ dyn/cm at 25 °C or below. In contrast, these films were all stable at higher surface pressures in the 30–40 °C range (see Table II, for example).

Discussion

In order to interpret the variety of experiments reported here we shall approach the results by considering first the associations within the crystals as reflected by melting points, enthalpies and entropies of fusion, and spectroscopic data. Secondly, we shall discuss associations within the film as reflected in surface equilibrium properties (equilibrium spreading pressures), Π/A curves, which in some cases are a mixture of thermodynamic and dynamic properties, and surface shear viscosities. Finally, various types of microscopic examination will be dealt with.

(24) Gaines, G. L. *Insoluble Monolayers at Liquid-Gas Interfaces*; Wiley-Interscience: New York, 1966; pp 281–286.

(25) (a) Schipper, P. E.; Harrowell, P. R. *J. Am. Chem. Soc.* **1983**, *105*, 723. (b) Craig, D. P.; Elsum, I. R. *Chem. Phys.* **1982**, *73*, 349.

(26) (a) Crisp, D. J. *Surf. Chem. (Suppl. Res. London)* **1949**, *17*. (b) Defay, R. Doctoral Dissertation, Brussels, 1932.

(22) Uzu, Y.; Sugiura, T. *J. Colloid Interface Sci.* **1975**, *51*, 346.

(23) Harkins, W. P.; Boyd, E.; Young, T. F. *J. Chem. Phys.* **1940**, *8*, 954.

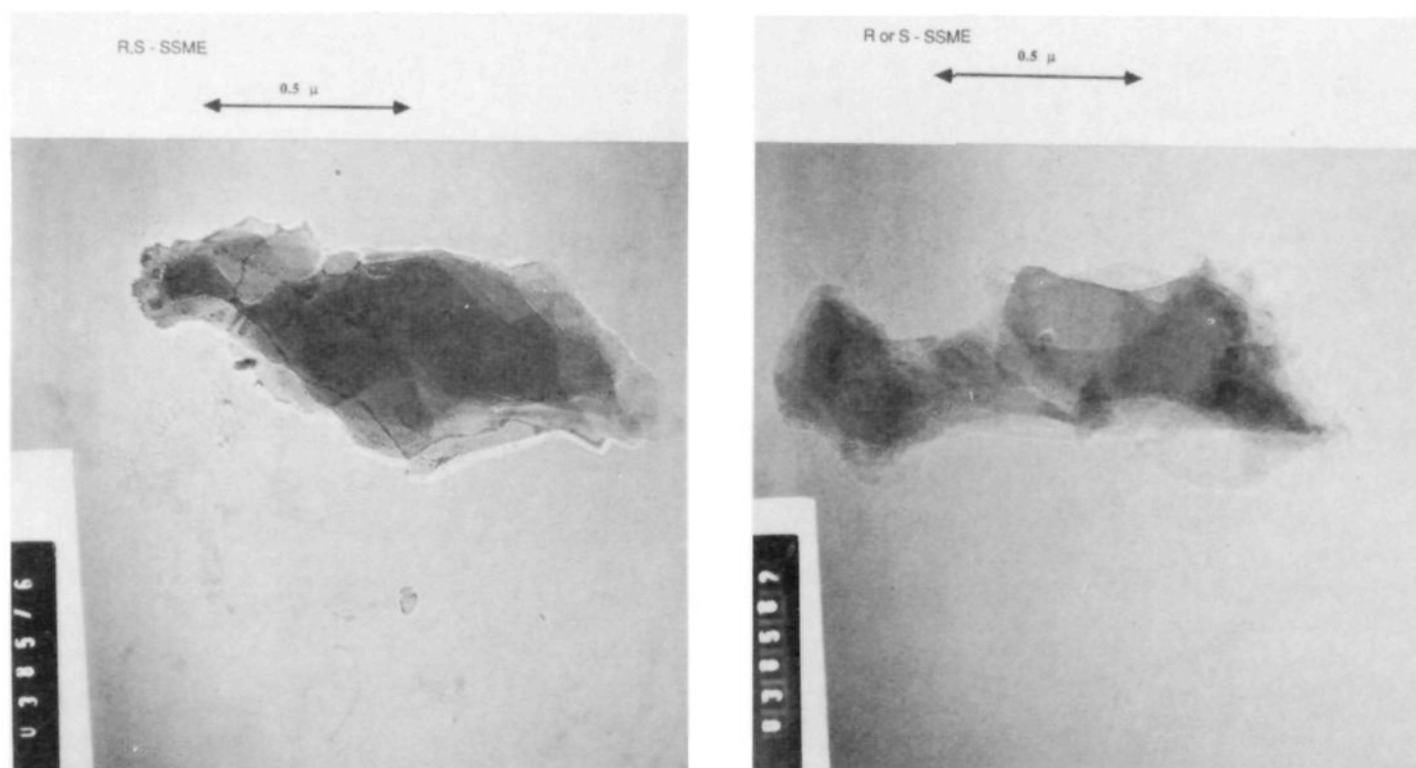
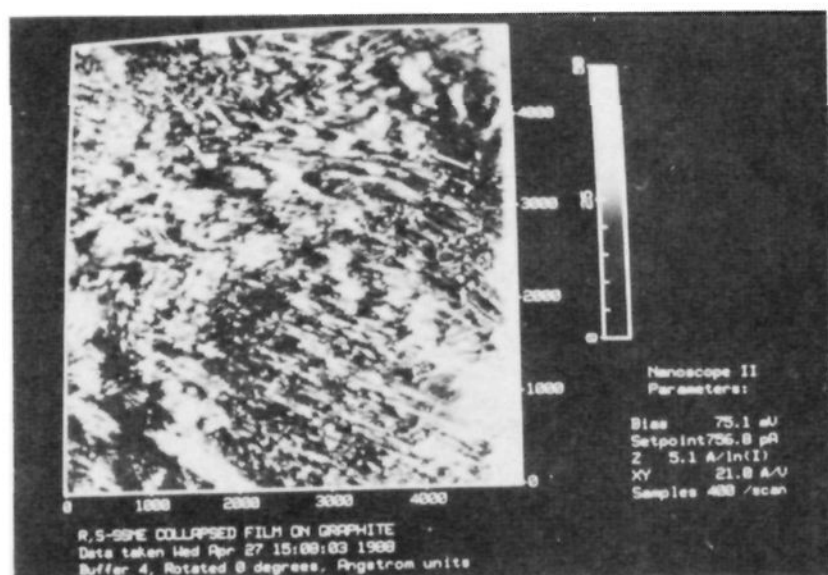


Figure 5. Transmission electron micrographs of L-B films of collapsed domains in racemic and enantiomeric SSME films pulled onto electron microscope specimen grids.

a) RACEMIC



b) ENANTIOMERIC

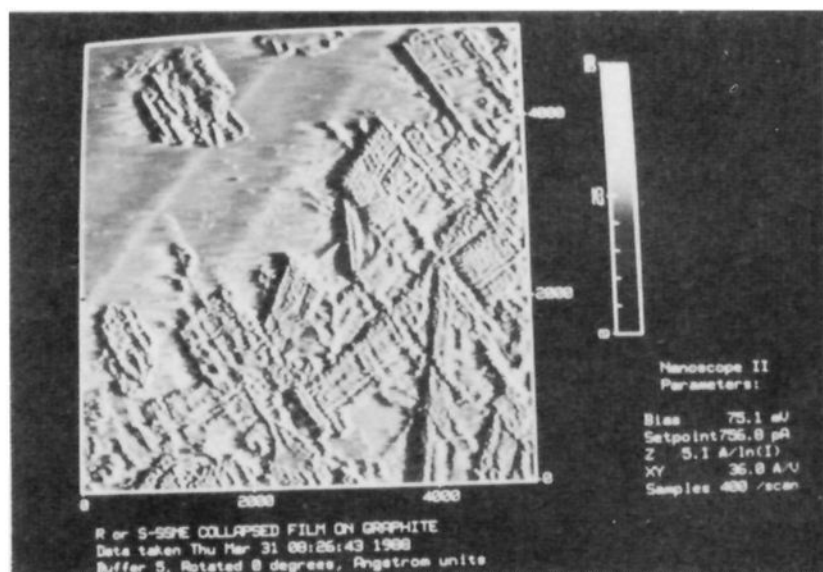


Figure 6. Scanning tunneling electron micrographs of L-B films of collapsed domains in (a) racemic and (b) enantiomeric SSME films pulled onto pyrolytic graphite monochromators. X and Y axes are in Å.

Association within the Crystalline Phase. The melting point diagram of Figure 2 shows that SSME forms a racemic compound or racemate in which there is a preference for R and S enantiomer packing as the lowest energy crystalline arrangement.²⁰ Successive incorporation of the R enantiomer into the S (or viceversa) crystalline phase results in a rise in crystal-lattice energy (or

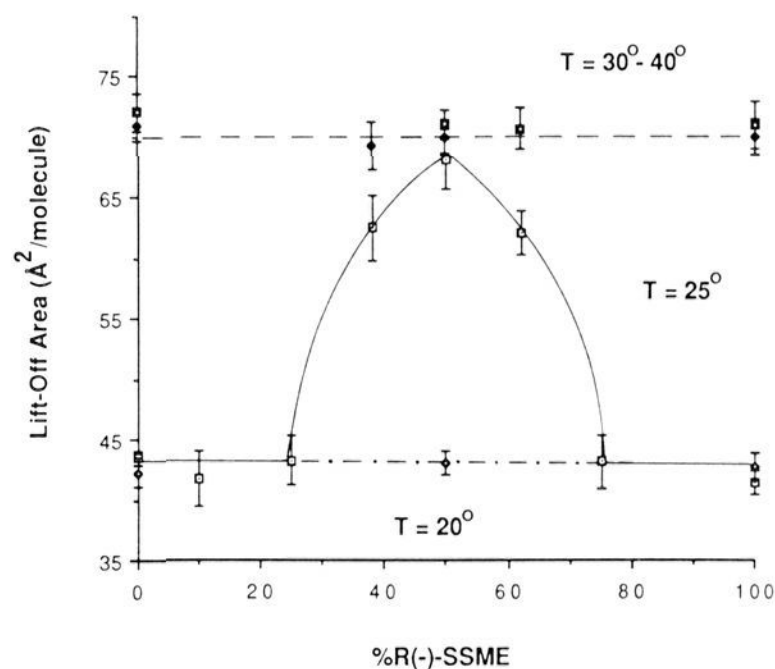


Figure 7. "Liftoff" area vs composition diagram for SSME films on pure water subphase at 20, 25, 30, and 40 °C.

lowering of T_{fusion}) until an enantiomeric excess of about 80%. At this point, a steady change in the crystalline packing results in a lowering of the lattice energy until a racemate is formed. It is interesting to note that despite the small (<4 °C) difference in the melting points of the enantiomeric and racemic crystals, the relative change in transition temperature upon enantiomer "mixing" is large, especially at greater than 60% enantiomeric excess.

The apparently early onset of eutectic formation indicates that the racemate is a stable one.²⁷ According to the general relationship below for determining racemate stability as described by

$$i = (T_{\text{Racemate}}^f - T_{\text{Eutectic}}^f) / (T_{\text{Enantiomer}}^f - T_{\text{Eutectic}}^f)$$

Petterson,²⁸ T^f is the temperature of fusion and i is an empirical measure of the tendency for compound formation. By this criterion SSME has a strong ($i > 1.5$) tendency to form a stable racemic compound.

The strength of the crystalline interactions is also reflected in the large enthalpies of fusion for the racemate and the enantiomeric crystals. Although the racemate has the higher melting point, its enthalpy of fusion is lower than that of the lower melting enantiomeric crystal. However, the decrease in entropy upon

(27) Jacques, J.; Collet, A.; Wilen, S. H. *Enantiomers, Racemates, and Resolutions*; Wiley: New York, 1981; pp 93-97.

(28) Petterson, K. *Ark. Kemi.* 1956, 10, 297.

fusion is about 18 cal/K mol *less* in the case of the racemate, suggesting a greater gain in entropy upon melting for the enantiomeric crystal despite its lower melting point. This points to the latter as being a more highly ordered crystalline array than the racemate. Similar stereochemically dependent melting properties have been observed with other *N*-acyl amino acid derivatives, and they have been found to be dependent on acyl chain length and hydrogen bonding.^{29,30}

Unfortunately, we were unable to grow crystals of the enantiomers or the racemic mixture of SSME of high enough quality to permit a full x-ray structure analysis. We know of no published structures of any amino acid methyl ester fatty acid derivatives, and unless the fatty acid chains were of comparable length to the stearyl derivatives, there would be no assurance that the crystal packing was that adopted by our compounds. Although there are many crystal structures of amino acids including serine,³¹ they are all in the zwitterionic form and the structures are dominated by hydrogen bonding between the ammonium and carboxylate groups, which of course is precluded for the esters. The strong associations implied by both melting points and enthalpies of fusion in SSME crystals are understandable on the basis of hydrogen bonding between hydroxyl, amide, and ester headgroups, but until there is a complete structure determination, it would be unwise to speculate on which interactions are primarily responsible for the observed energy differences.

The infrared spectrum of the racemic material shows a pronounced hydrogen-bonding broadening in the OH region that is absent in the enantiomers. In addition, there are significant differences in the frequencies of the amide I carbonyl stretch and the amide CH, CH₂ bending bands between enantiomeric and racemic crystals, indicating clear differences in packing about the chiral centers in both forms. Interestingly, the proton magnetic resonance of the enantiomers in deuteriochloroform shows non-equivalence of the methyl hydrogens on the carbon attached to the hydroxyl group implying *intramolecular* hydrogen bonding, presumably to the carbonyl oxygen of the ester group. However, this says very little concerning the *inter-* or *intramolecular* hydrogen bonding which would occur for the ester hydroxyl or amide functions within the crystal or when spread on the aqueous subphase, where any of these groups may be interacting with water or with other serine molecules, particularly at low areas/molecule. Since SSME shows the most pronounced chiral recognition of the amino acid methyl esters studied by us (alanine, tyrosine, tryptophan)³² it is reasonable to suppose that its hydroxyl group is somehow implicated in chiral organization in the crystal, the monolayer or both. Beyond that we cannot be more specific about structural factors in the two phases.

Associations within the Monolayer Film. Although we can compare some of the properties of the enantiomeric and racemic crystals and their physical state is clearly defined, the actual state of the spread film is in principle a much more complex affair. Ultimate interpretation of the film at the molecular level would have to deal with such questions as the following: (a) Which functionalities of the headgroup are on (or in) the surface? (b) What is the water surface like; how deep is it? (That is, how many water molecules below the uppermost liquid ones are in an environment that is different from those within the true liquid water subphase?) (c) How much is the water disrupted by putting the headgroup into it? (d) How much intermolecular interaction is there between the headgroup functionalities of the enantiomeric or racemic spread films? Unless all of these structural and energetic factors are known, one may only speculate about the molecular interactions of the headgroups with each other and with the aqueous subphase. In fact, so many reasonable structures may be drawn for these interactions that almost any interpretation could

be accommodated. With this problem in mind, we shall compare the observed surface thermodynamic and dynamic properties of racemic and enantiomeric SSME films, since they reflect directly the associations in a *continuum* of molecules which must arise ultimately as a function of molecular shape and symmetry.²⁵ However, we shall regretfully eschew any attempt to interpret the results in terms of detailed molecular models.

Figure 3 portrays the influence of temperature and composition on the force-area isotherms. Furthermore, in each case the expansion curve is shown in addition to the more traditional compression curve. The difference between these curves represents hysteresis—a warning that the compression isotherms cannot be treated strictly in terms of thermodynamic properties but are time-dependent and involve collapsed and/or metastable states. Chiral recognition is expressed strongly in the isotherms and hysteresis at 25 and 30 °C, but it is obviously quite sensitive to temperature variation. Comparison of Figure 3a–d indicates relatively similar behavior for the pure enantiomers at all three temperatures. The sudden onset of a steep increase in surface pressure as the area is decreased occurs at about the ESP (Table III) for the enantiomers at 20 and 25 °C, with a significant expansion at surface pressures below the ESP occurring at 30 °C. The behavior of the expansion curves is reproducible at all three temperatures, indicating a nearly constant average molecular area of 28–30 Å²/molecule as the film is reexpanded. These phenomena indicate a low compressibility indicative of a solidlike phase.

The behavior of the racemic monolayer is quite different. At 20 °C chiral discrimination is negligible, with the racemic mixture following virtually the same compression and expansion pathway as that of the enantiomers. However, at 25 and 30 °C the racemic mixture is much more expanded than the enantiomers and shows considerably more hysteresis. At 40 °C (Figure 3d) there is very little difference between the compression curves for the enantiomeric and the racemic mixture, both of which are highly expanded, but now only the enantiomeric films show considerable hysteresis when compressed over the monolayer stability limit.

Table II lists the variation in monolayer stability limits at 20, 25, 30, and 40 °C. Clearly, the enantiomeric film is less stable at all temperatures than the racemic film. Recalling that the ESPs of the enantiomers are much smaller than those of the racemate (Table III), we propose that all of the behavior we have described so far (the low ESP, the low film stability, the low compressibility above the monolayer stability limit) means that the enantiomeric film is collapsing to a more stable crystalline state than the racemic film and that it returns to that state more readily upon compression. However, as the temperature rises to 40 °C the factors that favor expansion override the tendency of the enantiomers to return to a crystalline or semicrystalline bulk phase on the surface. This process appears to be slow on the compression time scale, as suggested by the lack of any clear collapse point (i.e., a “kink” in the Π/A isotherm) that would indicate collapse to a solid, presumably bulk phase.

As a further comparison of dynamic behavior, Table IV presents surface shear viscosity results at the four temperatures and at two pressures. At 20 °C, where enantiomeric and racemic films show similar Π/A behavior, both films are too condensed to allow surface flow. At 30 °C and 2.5 dyn/cm surface pressure, enantiomeric films are more viscous due to the collapsed nature of the film, which leads to a non-Newtonian flow as compared to the fluid Newtonian flow of the racemic film. The same is true at $\Pi = 5.0$ dyn/cm, where the enantiomeric film is too collapsed to produce a steady flow rate. At 35 °C and 2.5 dyn/cm surface pressure, both films are stable and have the same shear viscosity within experimental error. At 5 dyn/cm, the enantiomeric film is again in a state of collapse and its flow is non-Newtonian. Finally, at 40 °C both films are stable at 2.5 and 5.0 dyn/cm and have the same shear viscosity, indicating that the fluid, liquidlike state of the film is independent of stereochemistry.

Figure 7 plots the “liftoff” area (the first point on the isotherm where the monolayers show detectable resistance to compression in a condensed phase) as a function of composition. At 20 °C

(29) Miyagishi, S.; Seichi, M.; Kazuhiko, M.; Asakawa, T.; Nishida, M. *Bull. Chem. Soc. Jpn.* **1985**, *58*, 1019.

(30) Miyagishi, S.; Seichi, M.; Tsuyoshi, A.; Nishida, M. *Bull. Chem. Soc. Jpn.* **1986**, *59*, 557.

(31) Frey, M. N.; Mogens, S. L.; Koetzles, T. F.; Hamilton, W. C. *Acta Crystallogr.* **1973**, *B29*, 876.

(32) Verblar, R. Ph.D. Dissertation, Duke University, Durham, NC, 1982.

there is no variation of "liftoff" area, and as we have seen there is very little difference in the compression and expansion behavior of the pure enantiomers or their mixtures. In addition, the films are too condensed to flow even for a 50/50 mixture. At higher temperatures (30–40 °C), again there is no significant difference between "liftoff" areas nor for any properties of the films below their stability limits. In terms of these properties the film behavior is nearly identical. The principal chiral differentiation at this point occurs at 25 °C, where the racemic mixture is much more expanded, much more fluid, and stable to a higher pressure than the pure enantiomeric films, as evidenced by film stabilities and viscosities.

We interpret this behavior as being primarily due to a simple mixing phenomenon by which the presence of two enantiomeric forms in their racemic mixture interferes with the formation of the closely packed arrangement of either pure enantiomer. At low pressures, where there is little interaction between surfactant molecules, there will be no opportunity for molecular recognition anymore than would be possible in a gas or dilute solution. At higher pressures a pure enantiomeric film reverts easily to its condensed closely packed quasicrystalline state. However, the presence of molecules of the opposite configuration increases the entropy (by at least the familiar $R \ln 2$ term), and thereby increases fluidity by perhaps as much as a simple achiral diluent would.

As stated earlier, the attempt at a complete analysis of the system must include what is happening in the aqueous subphase. In previous investigations of heat capacities of solution of various organic compounds in water, we have emphasized the important role that the enormous heat capacity of water contributes to hydrophobic phenomena.³³ It seems more than likely that the extraordinary temperature sensitivity of chiral discrimination shown in Figure 3a–d is a manifestation of the changing interaction of the headgroups and hydrocarbon chains with water over a modest temperature range. As a test of this proposal we have repeated several experiments using urea, a notorious "water structure breaker",³⁴ in the subphase. However, we have been unable to detect any effect of urea on the properties of either racemic or enantiomeric SSME films cast on subphases of ≤ 0.5 M urea. Although it has been proposed that water encapsulated in folded proteins is of significantly different structure than the bulk water,³⁵ it is not possible to deduce any difference in the

structure of the vicinal water layer(s) as a function of headgroup chirality from the experiments reported here.

Comparative Microscopy. The differences in the collapsed vs monolayer phases of these films as they reside on the water subphase at 25 °C is shown by epifluorescence micrographs (Figure 4), where racemic films form the spiraling, random arrays shown in the stable monolayer phase while the unstable enantiomeric film is apparently a condensed crystalline phase. The implied disorder of the racemic film relative to the enantiomeric is consistent with all the other monolayer data presented here. Langmuir–Blodgett transferred films pulled at surface pressures above the stability limits at 25 °C indicate clearly the presence of microcrystalline domains (Figure 5), and it appears from the scanning tunneling micrographs (Figure 6) that the packing within these domains is stereochemically dependent as would be expected for a crystalline phase. The enantiomeric surface microcrystalline domains appear *visually* to have a much higher degree of order than the racemic domains, which the entropies of fusion indicate to also be the case for the three-dimensional crystals.

Conclusions

All of the results reported here indicate that the films cast from the pure enantiomers of SSME go to a crystalline or quasicrystalline surface state at lower surface pressures than do the racemic films. In contrast, the racemic mixture shows a much higher degree of disorder and fluidity on the surface at higher surface pressures although a crystalline racemate is formed in the bulk phase. These conclusions, based on thermodynamic analysis of the monolayer properties, are supported strongly by microscopic examination using McConnell's epifluorescence microscopy technique in situ on the water surface, transmission electron microscopy, and scanning tunneling microscopy of the Langmuir–Blodgett films transferred to a graphite substrate. The latter provides an elegant view of long, linear escarpments approximately one molecular unit in height for the enantiomeric films. Furthermore, when both racemic and enantiomeric films are in stable, fluidlike states, there is no stereochemical dependence of any monolayer property which we have measured. Although molecular interactions in both the solid crystalline and monolayer phases are stereochemically dependent, it cannot be assumed that the structures or modes of intermolecular aggregation are the same in both phases.

Acknowledgment. This work was supported by NIH Grant No. RO1-GM28757 and a generous grant from AT&T. We are glad to acknowledge the assistance of Professor Harden McConnell, Vincent Moy, Professors Tim Oliver and Tom McIntosh, and Marjorie Richter.

(33) Arnett, E. M.; Mirajovsky, D. *J. Am. Chem. Soc.* **1982**, *105*, 1112.

(34) Finer, E. G.; Franks, F.; Tait, M. J. *J. Am. Chem. Soc.* **1972**, *94*, 4424.

(35) (a) Nozaki, V.; Tanford, C. *J. Biol. Chem.* **1971**, *246*, 2211. (b) Tanford, C. *Adv. Protein Chem.* **1968**, *23*, 121.